

Oxygen abundance distribution in the Galactic disc

S. A. Korotin,¹★ S. M. Andrievsky,^{1,2} R. E. Luck,³ J. R. D. Lépine,⁴ W. J. Maciel⁴
and V. V. Kovtyukh¹

¹*Department of Astronomy and Astronomical Observatory, Odessa National University and Isaac Newton Institute of Chile, Odessa Branch, Shevchenko Park, UA-65014 Odessa, Ukraine*

²*GEPI, Observatoire de Paris-Meudon, CNRS, Université Paris Diderot, F-92125 Meudon Cedex, France*

³*Department of Astronomy, Case Western Reserve University, 10900 Euclid Avenue, Cleveland, OH 44106-7215, USA*

⁴*Instituto de Astronomia, Geofísica e Ciências Atmosféricas da Universidade de São Paulo, Cidade Universitária, CEP: 05508-900, São Paulo, SP, Brazil*

Accepted 2014 August 10. Received 2014 August 10; in original form 2014 May 16

ABSTRACT

We performed a non-local thermodynamic equilibrium (NLTE) analysis of the infrared oxygen triplet for a large number of Cepheid spectra obtained with the Hobby–Eberly Telescope. These data were combined with our previous NLTE results for stars observed with the Max Planck Gesellschaft Telescope with the aim of investigating the oxygen abundance distribution in the Galactic thin disc. We found the slope of the radial (O/H) distribution to be equal $-0.058 \text{ dex kpc}^{-1}$. However, we found some evidence that the distribution might become flatter in the outer parts of the disc. This is supported by the results of other authors who have studied open clusters, planetary nebulae and H II regions. Some mechanisms of flattening are discussed.

Key words: stars: abundances – stars: variables: Cepheids – Galaxy: abundances – Galaxy: disc – Galaxy: evolution.

1 INTRODUCTION

From an astronomical point of view, oxygen is among the most interesting elements in the Universe. The reasons for this include the fact that it is the third most abundant element, it constitutes the base of life (at least on Earth), and it is used as a proxy of the global metal content in several astronomical objects – thus, when measured in objects with different ages, it is a tracer of the temporal evolution of the chemical content of our Galaxy. General information about the oxygen abundance distribution in Galactic substructures comes from the spectroscopic study of sources such as stars, planetary nebulae (PNe), H II regions and interstellar matter. Comparison of the data on oxygen abundance provided by these sources shows that there are discrepancies that affect our understanding of those processes that are responsible for the production and distribution of this element in our Galaxy and other galaxies. Thus new accurate oxygen abundance data from a large homogeneous sample of objects at different Galactocentric distances are urgently needed.

Because oxygen and other α -elements are produced in explosive processes in Type II supernovae (SNe II), it is of particular interest to study the distribution of oxygen in the Galactic thin disc. The characteristics of such a distribution may reveal the spatial pattern of SNe II activity, which we believe is influenced by the interstellar gas density distribution in the disc, by the effect of the Galactic spiral arms on the gas, and by the local metallicity level.

Studies of the elemental abundance gradients with Galactic Cepheids reveal growing evidence that elemental distributions in the disc require for their description not a single-slope gradient but rather a bimodal (or even multimodal) structure with different slopes in each region. For instance, Andrievsky, Bersier & Kovtyukh (2002b), using a sample of Cepheid stars, demonstrated that compared with other α - and iron-group elements, oxygen and iron show a steeper increase of their content towards the Galactic Centre. This increase at about 6.6 kpc corresponds to a change from the flat distribution in the solar vicinity to a much steeper one in the range $\sim 4\text{--}7$ kpc. This is supported by the results for the iron distribution found by Pedicelli et al. (2009) and Genovali et al. (2013).

Later, Luck, Gieren & Andrievsky (2003) reported a clear separation in elemental abundance distributions in the outer Galactic disc from those in its middle part. This separation is associated with a Galactocentric distance of about 10 kpc. This finding was confirmed by Andrievsky et al. (2004) with a larger sample of stars. They concluded that ‘the wriggle feature in the metallicity distribution, which is associated with Galactocentric distance of about 11 kpc can be interpreted as a change of metallicity level in vicinity of the Galactic corotation resonance’.

In contrast, Kovtyukh, Wallerstein & Andrievsky (2005) and Luck, Kovtyukh & Andrievsky (2006) did not find a good reason not to use a simple linear gradient to describe the spatial abundance distributions obtained with an even larger sample of Cepheid stars. The same conclusion was reached by Luck et al. (2011) and Luck & Lambert (2011) (but they noted an increased scatter of the

★E-mail: serkor@skyline.od.ua

abundance data beyond a distance of 10 kpc). This conclusion may be affected by the inclusion of new Cepheids covering more distant parts of the disc in Galactocentric longitude, which could obscure any features in the radial abundance distribution.

Genovali et al. (2014) also used a single gradient value to describe the iron abundance distribution over a broad range of Galactocentric distances from 5 to 19 kpc. Lemasle et al. (2013) also do not support the flattening of the abundance distribution for some elements in the outer Galactic disc, but they do not provide the corresponding data for oxygen and iron.

Thus the characteristics of the abundance distributions of astrophysically important elements such as oxygen and iron in the Galactic disc are far from being clear. All the data on the oxygen distribution from giant and supergiant F-G-K stars come from analysis of either forbidden oxygen lines at 630.03 and 636.38 nm or the 615.6–615.8 nm triplet, but there are known problems regarding the reliability of the oxygen abundance determination from this restricted sample of lines. For example, two forbidden lines can hardly be detected in supergiant spectra if the effective temperature of the star is higher than 5500 K, but this is the case for a large number of Cepheids. Moreover, these lines are often polluted with terrestrial absorptions. Because this region is dominated by terrestrial bands, additional spectrum cleaning is needed. Among the triplet lines, only the line at 615.8 nm is more or less detectable in supergiant spectra. It cannot be detected in the medium-to-high resolution spectra of stars with effective temperature lower than 5500–6000 K. Thus, in some cases, in order to derive the oxygen abundance for a large sample of Cepheid stars it is necessary to use either forbidden lines (for cooler stars, or for phases of minimum with lower temperature), or triplet lines (for the hotter stars).

A good solution would be to use the 777.1–777.4 nm triplet. It affords the best opportunity to derive oxygen abundance in F-G-K supergiants because: (1) its lines are quite strong and very well shaped over a wide range of the effective temperature; (2) these lines are hardly blended; (3) the lines are reachable with many spectrographs, even for the faintest Cepheids. The most significant obstacle that prevents the wide use of this triplet in spectroscopic analyses is the obvious need to apply a sophisticated non-local thermodynamic equilibrium (NLTE) approximation in order to obtain the correct oxygen abundance. This is a well-known problem (see, for example, the very instructive example detailing the extremely strong dependence of the derived oxygen abundance on the effective temperature provided in the LTE study of Schuler et al. 2006).

The main goal of the present paper is to derive the correct NLTE oxygen abundance for a large homogeneous sample of Cepheids using the infrared (IR) oxygen triplet, and then on this basis to construct the oxygen abundance distribution in the Galactic thin disc.

The paper is organized as follows. Our sample of Cepheids is presented in Section 2. The NLTE approximation that was used to derive the oxygen abundance from the strong IR triplet is described

in detail in Section 3. The oxygen abundance distribution in the disc is the subject of Section 4. The Discussion and Conclusion in Sections 5 and 6 summarize our results from the point of view of recent observational and theoretical works on abundance gradients in the Galactic disc.

2 OUR SAMPLE OF STARS

Continuing our program of the investigation of the Galactic abundance gradient (Andrievsky et al. 2002a,b,c; Luck et al. 2003; Andrievsky et al. 2004; Luck et al. 2006; Lépine et al. 2011), we study the oxygen distribution in the thin disc with a large sample of Galactic Cepheids. Our sample consists of two subsamples. One contains the Hobby–Eberly Telescope (HET) data, described in detail by Luck & Lambert (2011). The second comprises the Max Planck Gesellschaft (MPG) Telescope data, which are described in Luck et al. (2013). The observational data for both samples were collected by one of the authors (REL). The list of the studied stars (HET data only) and their spectra can be found in Table 1 (full form available online).

3 METHOD OF ANALYSIS

The NLTE approximation was used to derive the oxygen abundance in our stars. For this we used the O I triplet at 777.4 nm. The NLTE deviations in the IR oxygen triplet have previously been studied by many authors (e.g. Kiselman 1991; Takeda 1992; Carlsson & Judge 1993; Paunzen et al. 1999; Reetz 1999; Mishenina et al. 2000; Przybilla et al. 2000; Fabbian et al. 2009; Sitnova, Mashonkina & Ryabchikova 2013). As shown by these authors, NLTE effects significantly strengthen these lines. At the same time, available O I atomic models were not always able to reproduce observed triplet profiles. For instance, Przybilla et al. (2000) found different oxygen abundances in A and F stars as derived from IR lines and from lines in the visual part of the spectrum.

The most complete atomic models published by Sitnova et al. (2013) and Fabbian et al. (2009) take into account the most recent collision-rate values between atoms and electrons (Barklem 2007). However, the lack of detailed calculations describing collisions with hydrogen atoms necessitates the use of Drawin’s formula (Drawin 1969) with a very uncertain correcting factor varying from 0 to 1.

In this work we modify our oxygen atomic model first presented in Mishenina et al. (2000) and then updated in Dobrovolskas et al. (2014). Our present model consists of 51 O I levels of singlet, triplet and quintet systems and the ground level of the O II ion. An additional 24 levels of neutral oxygen and 15 levels of ions in higher states are added for particle number conservation. The Grotrian diagram of our model is shown in Fig. 1. Fine-splitting was taken into account only for the ground level and 3p5P level (the upper level for the 777.4-nm triplet).

Table 1. Parameters and abundances for program Cepheids. Stellar parameters: T_{eff} , effective temperature; $\log g$, logarithm of surface gravity; V_t , microturbulent velocity; (Fe/H), iron abundance; (O/H), oxygen abundance; R_G , Galactocentric distance. Only the first few lines are shown: the full table is available online.

Object	Phase	T_{eff} [K]	$\log g$	V_t [km s ⁻¹]	(Fe/H)	(O/H)	R_G (kpc)
AA Gem	0.422	5141	1.23	3.92	7.34	8.51	11.55
AA Gem	0.658	5190	1.45	5.85	7.38	8.51	11.55
AA Mon	0.841	5797	2.26	4.90	7.41	8.51	11.36

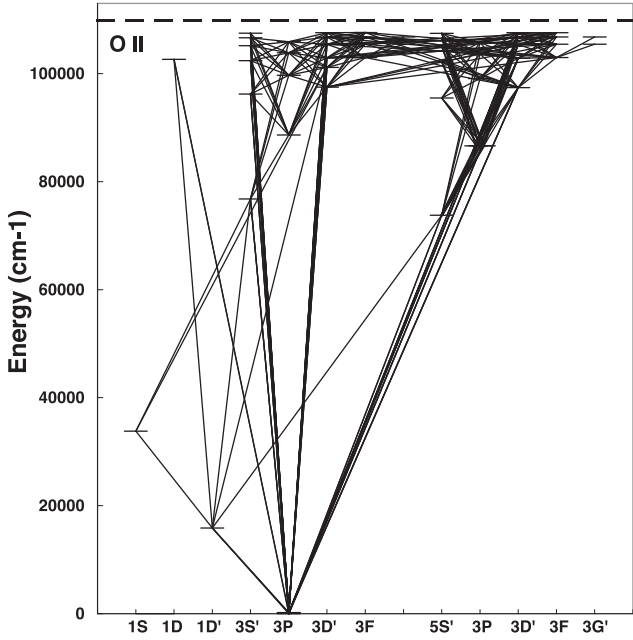


Figure 1. The Grotrian diagram for O I.

A total of 248 bound–bound transitions were included in the detailed analysis. Photoionization cross-sections were selected from TOPBASE (Cunto et al. 1993). Accurate quantum mechanical calculations were employed for the first 19 levels to find collision rates with electrons (Barklem 2007). Using spline interpolation, the collision rates can be interpolated against temperature. The remaining allowed collisional transitions were approximated by the van Regemorter (1962) formula, while for the forbidden transitions we applied Allen’s (1973) formula with the collision strength set equal to 1.0. Collisions with hydrogen atoms were described using Drawin’s formula (Drawin 1969), as modified by Steenbock & Holweger (1984). An oscillator strength of $f = 0.001$ was used for the forbidden transitions (Fabbian et al. 2009). Generally, our model is similar to that of Sitnova et al. (2013). The MULTI code (Carlsson 1986) was used to compute NLTE level populations. This code was modified by Korotin, Andrievsky & Luck (1999).

As shown by Sitnova et al. (2013), in order to achieve agreement between the oxygen abundances in A stars derived from IR triplet lines, and from lines in the visual part of the spectrum, it is necessary to decrease the collision rates calculated by Barklem (2007) by a factor of four. In order to adjust oxygen abundances from different multiplets in the solar spectrum, and in the Vega spectrum, they adopted a correcting factor in Drawin’s formula of $S_H = 1$. We performed test calculations for Vega and Sirius using our oxygen atom model and found that it is not possible to describe observed line profiles for different multiplets with a single oxygen abundance value. While the O I triplet at 615.7 nm is almost free of the influence of NLTE, the lines of the triplet at 777.4 nm appear to be weaker than the observed ones.

If we decrease the collision rates calculated by Barklem (2007) by a factor of four times, as done by Sitnova et al. (2013), we can fit the observed profiles for these two triplets with a single abundance, but the synthetic lines of another IR triplet at 844.6 nm appear to be significantly increased compared with observations. This is seen even in the Procyon spectrum, although in its cooler atmosphere the collisions with hydrogen atoms begin to be more important.

For our test calculations we used the same stellar parameters and oxygen abundance as Sitnova et al. (2013). Table 2 lists the sources of the observed spectra and stellar parameters.

We consider that a decrease of all collision rates calculated by Barklem (2007) is not appropriate; therefore, we decided to change the collision rates only for some transitions. Thus, we decreased by a factor of two the rates that correspond to the IR triplet at 777.4 nm, and increased by four times the rates that correspond to the 884.6-nm triplet. We also strengthened the coupling between the 3p3P level (the upper level for the 844.6-nm triplet lines) and levels of the quintet system 4s5S⁰ and 3d5D⁰ owing to collisions with hydrogen atoms. For the forbidden transitions we used $f = 1.0$ in Drawin’s formula. With these modifications, we were able to adjust the theoretical and observational profiles of oxygen lines of different multiplets in the spectra of the rather hot A–F stars, the solar-type stars as well as the cooler stars. For the cooler stars we used the correcting factor $S_H = 1$, in agreement with Fabbian et al. (2009) and Sitnova et al. (2013).

In Fig. 2 we show a comparison between observed and synthetic profiles for the lines of various multiplets for Vega and Procyon. Note that a single oxygen abundance value was used to synthesize all the lines for each star. Good agreement is seen both for the 615.7-nm triplet lines, which are not affected significantly by NLTE effects, and for the IR triplets, which are significantly affected. Another test was applied to the solar spectrum. We used the solar atmosphere model of Castelli & Kurucz (2003), supplemented by the VAL-C chromosphere model (Vernazza, Avrett & Loeser 1981) with an explicit distribution of the microturbulent velocity. (Note that the influence of the chromosphere on the lines of IR triplets is very small, no more than 1.5 per cent in their equivalent widths.) Observed profiles were taken from the Solar flux atlas (Kurucz et al. 1984). We also made a comparison for the solar disc centre using the Solar atlas of Delbouille, Roland & Neven (1973). A comparison of the theoretical profiles for the 630-nm line and the lines of the 777.4- and 844.6-nm triplets with observed profiles in the solar spectrum is shown in Fig. 3. In order to synthesize all the lines we used a single oxygen abundance $\log \epsilon(O) = 8.71$ (the same value as proposed by Scott et al. 2009).

The results of NLTE oxygen abundances for the HET stars are given in Table 1. We also list the parameters of the stars (effective temperature, surface gravity, microturbulent velocity) as derived by Luck & Lambert (2011) for the HET sample. Our NLTE data for the stars of the MPG set can be found in Luck et al. (2013), while atmosphere parameters and LTE abundances for those stars are available in Luck et al. (2011). Galactocentric distances for our program stars were calculated in the same way as in Andrievsky et al. (2002a). We used 7.9 kpc for the solar Galactocentric radius

Table 2. Stellar parameters.

Star	T_{eff} [K]	$\log g$	[Fe/H]	V_t [km s ⁻¹]	(O/H)	Res.	Source
Sun	5777	4.44	0.0	1.0	8.71	350 000	Kurucz et al. (1984)
Procyon	6590	4.00	0.0	1.8	8.73	80 000	Bagnulo et al. (2003)
Vega	9550	3.95	-0.5	2.0	8.59	100 000	Takeda, Kawonomoto & Ohishi (2007)
Sirius	9850	4.30	0.4	1.8	8.42	80 000	Bagnulo et al. (2003)

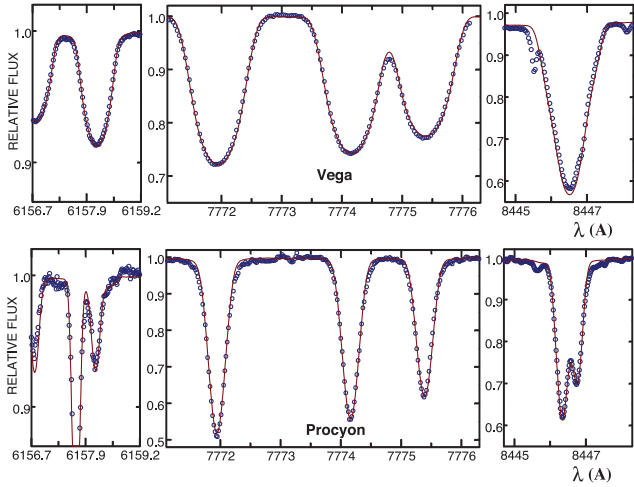


Figure 2. Profile fitting of the O I line in the Vega and Procyon spectra.

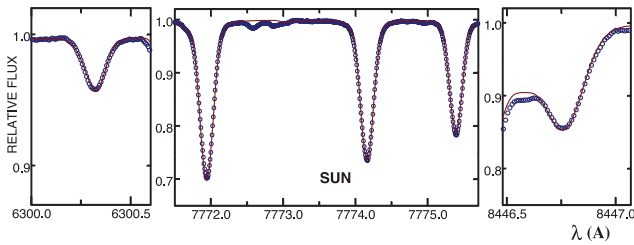


Figure 3. Profile fitting for the oxygen lines in the solar spectrum.

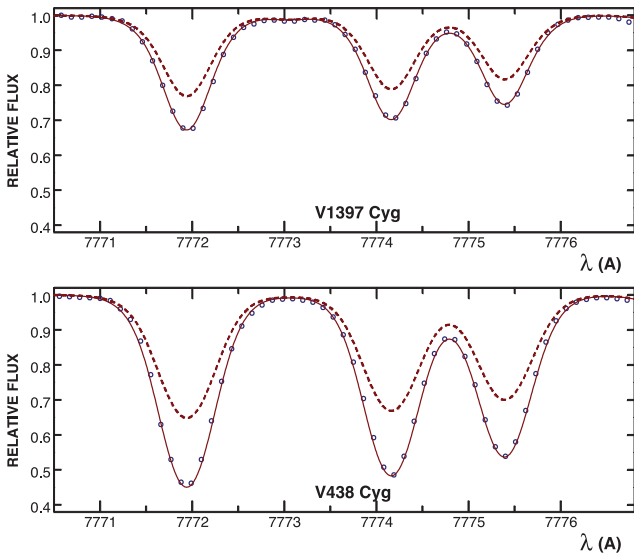


Figure 4. Profile fitting of the O I line in the Cepheid spectrum. Open circles, observed profiles; solid line, non-local thermodynamic equilibrium (NLTE) profiles; dashed line, LTE profiles calculated with the derived NLTE oxygen abundance.

(McNamara et al. 2000). If we compare our NLTE values with LTE values from Luck & Lambert (2011) and Luck et al. (2011) star-by-star, we obtain the following result: NLTE–LTE = -0.03 ± 0.13 (LTE results are based on the 615.6-nm line and the 630.0-nm forbidden line). The best fit of the NLTE synthetic profiles and observed profiles for some stars are given in Fig. 4. The NLTE corrections in this case are extremely strong, occasionally reaching

0.8–1.0 dex (the larger corrections are for stars with higher effective temperatures and lower gravity).

4 OXYGEN ABUNDANCE DISTRIBUTION IN THE DISC

In Fig. 5 we show the NLTE oxygen distribution versus Galactocentric distance for the combined sample of HET and MPG Telescope stars.

The region 5–13 kpc is well sampled by our oxygen data and the distribution is quite tight. At larger distances the data are more dispersed. Samples observed with different telescopes produce results that agree well.

The data in Fig. 5 can be interpolated linearly. In this case we have the slope $\Delta(\text{O}/\text{H})/\Delta R_G = -0.058$ with $R^2 = 0.61$. The slope derived by Luck & Lambert (2011) is similar: -0.056 with $R^2 = 0.47$. Those authors did not discuss the possible bimodal character of the gradient.

However, despite the less populated outer disc region, it seems that the abundance distribution here could be flatter. In Fig. 6 we show the same data as in Fig. 5, but assuming a bimodal distribution. We formally adopted the position of the possible break in

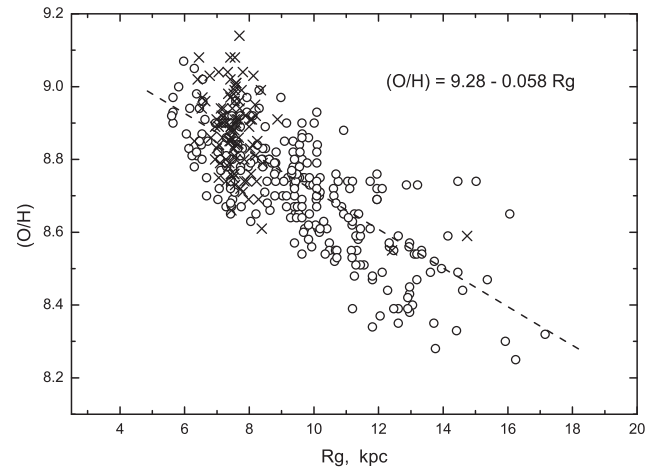


Figure 5. Non-local thermodynamic equilibrium oxygen abundance versus Galactocentric distance. Open circles, HET data; crosses, MPG Telescope data.

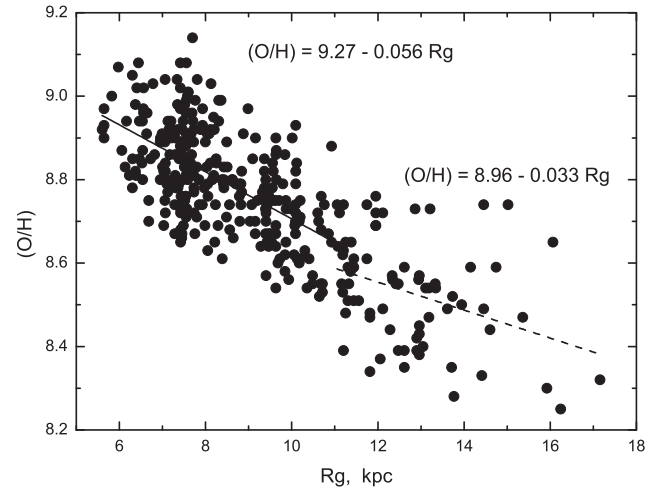


Figure 6. Bimodal distribution of oxygen abundance. The break position is close to 11 kpc.

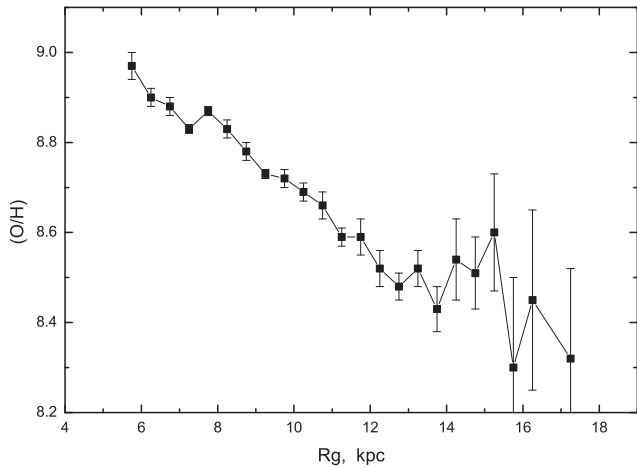


Figure 7. Oxygen abundance distribution (binned data).

the distribution at 11 kpc, taking into account that in many studies that report gradient flattening, distances of 10–12 kpc are mentioned (see references in the Introduction and Discussion).

A more robust confirmation of this conclusion follows from Fig. 7. In this figure all Cepheids were binned with a step of 0.5 kpc. For each bin we show the error of the mean. If only one star falls in a bin, then the error of the mean was adopted to be equal to 0.2. A clear change of the general trend at about 12 kpc and a local increase of the oxygen abundance in the vicinity of 15 kpc are seen.

5 DISCUSSION

As shown by Barros, Lépine & Junqueira (2013), the specific action of the corotation resonance results in the orbital trajectory migration of stars and also in the formation of a gas density minimum at the corotation radius. For instance, their fig. 7 demonstrates how a star initially located inside the corotation circle appears outside it after some time. A star initially outside the corotation circle, in contrast, migrates to inside it. The typical time of this change is about 2 Gyr. The star migration process itself may disturb the observed radial metallicity distribution at the present time.

More massive stars (such as Cepheid progenitors) have insufficient time to migrate far from their locations of birth, and therefore this mechanism is not efficient in modifying the metallicity distribution obtained from these objects. Their position should be approximately associated with their parent gas clouds. Because the gas component flows in the both direction from the corotation circle (with respect to stars) owing to the influence of angular momentum loss and gain in the vicinity of the corotation circle (Barros et al. 2013 and references therein), some increase in the metallicity can be expected outside the corotation circle, which reflects a local increase in the gas density, the star formation rate, and therefore the metallicity production. An element such as oxygen, being produced by massive short-lived stars, may show an abundance distribution that reflects the instantaneous mass density distribution in the Galactic disc. In our Fig. 6, a peculiar region could be associated with $R_G \approx 11$ kpc. Barros et al. (2013) find evidence of a mass density gap at a Galactocentric distance of about 9 kpc. This is somewhat less than 11 kpc, but qualitatively the conclusion remains the same.

If we turn to the iron abundance distribution using the most complete data for Cepheids provided by Luck & Lambert (2011), their fig. 1, then it is difficult to detect any peculiar point in this distri-

bution. Iron is efficiently produced by SNe Ia, whose progenitors have a typical lifetime of about 1 Gyr, or slightly longer (Iben & Tutukov 1984), which is comparable to the characteristic crossing time of the particular region in the vicinity of the corotation circle. The movement of the slightly larger number of SNe Ia progenitors from the inner part of the corotation circle towards the outer part, and the opposite movement of the smaller number of such stars from the outer part could increase the gas pollution with iron at the corotation circle itself and in the vicinity of it, and therefore veil any ‘instantaneous’ distribution picture of this element created by SNe II.

It should be noted that Daflon & Cunha (2004), based on observations of OB stars, found a different behaviour of the oxygen gradient from that in the present work, with a strong step near the solar radius (taken as 8.5 kpc). Massive OB stars are much younger (their ages do not exceed a few million years) than the Cepheids, so that in principle their abundance is really that of the surrounding gas. Costa, Uchida & Maciel (2004) derived some flattening at Galactocentric distances larger than 10 kpc on the basis of a set of Galactic PNe, and a previous paper in this series (Andrievsky et al. 2004, 2013) led to the same conclusion based on Cepheid variables. More recent results by Lemasle et al. (2013) suggest a constant slope along the Galactic radius, although their data are not inconsistent with some flattening at large Galactocentric distances. More recent results from the same group based on accurate iron abundances of a large sample of Galactic Cepheids (Genovali et al. 2014) are consistent with a linear gradient over a broad range of Galactocentric distances given by $-0.06 \text{ dex kpc}^{-1}$, very similar to the results shown in Fig. 5.

Open cluster data seem to indicate the same tendency as presented in this paper, as recently discussed by Yong, Carney & Friel (2012) based on α - and iron-group element abundances of a new sample of objects in the outer Galactic disc. For instance, the plot for representative α -element magnesium shows a break of the distribution at 13 kpc, with some flattening of the distribution at larger radii (see their fig. 31a). In principle, a similar behaviour is inherent in the Cepheid (Mg/H) distribution (fig. 31d).

The same conclusion was also reached by Magrini et al. (2009), who claimed that there is a flattening of the iron and α -element distribution (or even a plateau) at radii greater than 12 kpc. Cescutti et al. (2007) succeeded in modelling the flattening of the gradients produced by open clusters, as well as by Cepheids, hot stars and red giant stars.

Lépine et al. (2014) performed an average of abundances of several α -elements in order to decrease the effect of individual errors on measurements, and suggest (their fig. 6) that there are two distinct levels of α abundances, with some overlap in Galactic radius.

A recent study based on Galactic H II regions and featuring the outer-disc object NGC 2579 (Esteban et al. 2013) is also consistent with a flattened gradient at large distances from the Galactic Centre.

The flattening of gradients at large Galactocentric distances seems to be a universal property of disc galaxies. For example, Stasinska et al. (2013) considered PNe and H II regions in the spiral galaxy NGC 300 and found that oxygen and other element abundance gradients from PNe are significantly shallower than those from H II regions, and this may indicate a steepening of the metallicity gradient in NGC 300. A very clear flattening of the oxygen abundance distribution in the outer parts of the spiral galaxy M83 was reported by Bresolin et al. (2009) (see their fig. 9). Recently, Sanchez et al. (2014) presented the largest and most homogeneous catalogue of H II regions in several hundreds of galaxies from the

CALIFA survey. Many of these galaxies show a flattening in the oxygen abundance.

These results may in principle be affected by the time variation of the radial abundance gradients in the Galactic disc, but some recent work based on four different samples of Galactic PNe suggest that this variation has probably been very small during the past 4 to 5 Gyr, so that the gradients indicated by these different objects are essentially indistinguishable (Maciel & Costa 2013). Therefore, the PN gradient is not expected to be very different from the gradient observed in H II regions and Cepheid variables, an expectation that is supported by recent additional observational data on these objects (Fu et al. 2009; Pedicelli et al. 2009). Dynamical calculations valid for the Milky Way disc over a time span of about 6 Gyr seem to confirm these results (Curir et al. 2014).

In addition, some recent work on the time variation of the abundance gradients as a function of redshift suggest that the variations are indeed very small for $z < 0.5$ (cf. Pilkington et al. 2012; Gibson et al. 2013), which is the age bracket for most of the objects mentioned above.

Alternatively the data at Galactocentric distances larger than 14 kpc may in principle become more scattered. In such a case, the outer parts of the Galaxy may show abundances that reflect local events that influence the abundances more than the coherent evolution as implied by a gradient. Unfortunately, this type of analysis is not really possible with Cepheids (owing to the natural lack of Cepheid stars at large distances). Perhaps in the future giants might be used to continue the project.

6 CONCLUSION

Summarizing our present study, it is clear that there is growing observational evidence for the flattening of α -element distributions (including oxygen) in the discs of a number of galaxies, including our own. These data come from spectroscopic analyses of open clusters, PNe, H II regions, hot stars, red giant stars, and, now, from Cepheids.

Because oxygen is produced by massive short-lived stars, its abundance distribution should follow an instantaneous gas distribution in the Galactic disc. As recently concluded by Barros et al. (2013), based on several previous theoretical studies, the radial gas density profile has a gap at the corotation circle, and an increased density on both sides of it. Our observational data comprising a large sample of Cepheids, analysed taking into account NLTE effects on oxygen abundance determinations, seem to support this assumption, and show that the corotation resonance in the Galactic disc can have a significant impact on the abundance gradients in its vicinity. In particular, our oxygen abundance distribution reveals a clear change of the general trend at about 12 kpc, with subsequent flattening in the range from 12 to 15 kpc, or even a small increase of the oxygen abundance towards 15 kpc.

ACKNOWLEDGEMENTS

SAK and SMA acknowledge financial support from SCOPES grant no. IZ73Z0-152485. The authors thank the anonymous referee for her/his valuable comments that significantly improved the paper.

REFERENCES

Allen C. W., 1973, *Astrophysical Quantities*. Athlone Press, London
 Andrievsky S. M. et al., 2002a, *A&A*, 381, 32
 Andrievsky S. M., Bersier D., Kovtyukh V. V., 2002b, *A&A*, 384, 140

Andrievsky S. M., Kovtyukh V. V., Luck R. E., Lépine J. R. D., Maciel W. J., Beletsky Yu. V., 2002c, *A&A*, 392, 491
 Andrievsky S. M., Luck R. E., Martin P., Lépine J. R. D., 2004, *A&A*, 413, 159
 Andrievsky S. M., Lépine J. R. D., Korotin S. A., Luck R. E., Kovtyukh V. V., Maciel W. J., 2013, *MNRAS*, 428, 3252
 Bagnulo S., Jehin E., Ledoux C., Cabanac R., Melo C., Gilmozzi R., 2003, The ESO Paranal Science Operations Team, *Messenger*, 114, 10
 Barklem P. S., 2007, *A&A*, 462, 781
 Barros D. A., Lépine J. R. D., Junqueira T. C., 2013, *MNRAS*, 435, 2299
 Bresolin F., Ryan-Weber E., Kennicutt R. C., Goddard Q., 2009, *ApJ*, 695, 580
 Carlsson M., 1986, *Upps. Astron. Obs. Rep.*, 33, 1
 Carlsson M., Judge P. G., 1993, *ApJ*, 402, 344
 Castelli F., Kurucz R. L., 2003, in Piskunov N. E., Weiss W. W., Gray D. F., eds, *Proc. IAU Symp. 210, Modelling of Stellar Atmospheres*. Astron. Soc. Pac., San Francisco, poster A20 (CD-ROM); synthetic spectra, available at: <http://cfaku5.cfa.harvard.edu/grids>
 Cescutti G., Matteucci F., Francois P., Chiappini C., 2007, *A&A*, 462, 943
 Costa R. D. D., Uchida M. M. M., Maciel W. J., 2004, *A&A*, 423, 199
 Cunto W., Mendoza C., Ochsenbein F., Zeippen C. J., 1993, *A&A*, 275, L5
 Curir A., Serra A. L., Spagna A., Lattanzi M. G., Fiorentin P. Re, Diaferio A., 2014, *ApJ*, 784, L24
 Daflon S., Cunha K., 2004, *ApJ*, 617, 1115
 Delbouille L., Roland G., Neven L., 1973, *Atlas Photométrique du Spectre Solaire de λ 3000 à λ 10000 Å*. Institut d'Astrophysique, Univ. Liege
 Dobrovolskas V. et al., 2014, *A&A*, 565, 121
 Drawin H. W., 1969, *Z. Phys.*, 225, 483
 Esteban C., Carigi L., Copetti M. V. F., Garcia-Rojas J., Mesa-Delgado A., Castaneda H. O., Pequignot D. M., 2013, *MNRAS*, 433, 382
 Fabbian D., Asplund M., Barklem P. S., Carlsson M., Kiselevich D., 2009, *A&A*, 500, 1221
 Fu J., Hou J. L., Yin J., Chang R. X., 2009, *ApJ*, 696, 668
 Genovali K. et al., 2013, *A&A*, 554, 132
 Genovali K. et al., 2014, *A&A*, 566, 37
 Gibson B. K., Pilkington K., Bailin J., Brook C. B., Stinson G. S., 2013, XII Intern. Symp. Nuclei in the Cosmos (NIC XII), available at: <http://pos.sissa.it/cgi-bin/reader/conf.cgi?confid=146>, id. 190
 Iben I., Jr, Tutukov A. V., 1984, *ApJ*, 284, 719
 Kiselevich D., 1991, *A&A*, 245, L9
 Korotin S. A., Andrievsky S. M., Luck R. E., 1999, *A&A*, 351, 168
 Kovtyukh V. V., Wallerstein G., Andrievsky S. M., 2005, *PASP*, 117, 1173
 Kurucz R. L., Furenlid I., Brault J., Testerman L., 1984, *Solar Flux Atlas from 296 to 1300 nm*. National Solar Observatory, Sunspot, New Mexico
 Lemasle B. et al., 2013, *A&A*, 558, A31
 Lépine J. R. D. et al., 2011, *MNRAS*, 417, 698
 Lépine J. R. D., Andrievsky S. M., Barros D. A., Junqueira T. C., Scarano S., Jr, 2014, in Feltzing S., Zhao G., Walton N., Whitelock P., eds, *IAU Symp. 298, Setting the Scene for GAIA and LAMOST*. Cambridge Univ. Press, Cambridge, p. 86
 Luck R. E., Lambert D. L., 2011, *AJ*, 142, 136
 Luck R. E., Gieren W. P., Andrievsky S. M., 2003, *A&A*, 401, 939
 Luck R. E., Kovtyukh V. V., Andrievsky S. M., 2006, *AJ*, 132, 902
 Luck R. E., Andrievsky S. M., Kovtyukh V. V., Gieren W., Graczyk D., 2011, *AJ*, 142, 51
 Luck R. E., Andrievsky S. M., Korotin S. N., Kovtyukh V. V., 2013, *AJ*, 146, 18
 Maciel W. J., Costa R. D. D., 2013, *Rev. Mex. Astron. Astrofis.*, 49, 333
 McNamara D. H., Madsen J. B., Barnes J., Ericksen B. F., 2000, *PASP*, 112, 202
 Magrini L., Sestito P., Randich S., Galli D., 2009, *A&A*, 494, 95
 Mishenina T. V., Korotin S. A., Klochkova V. G., Panchuk V. E., 2000, *A&A*, 353, 978
 Paunzen E. et al., 1999, *A&A*, 345, 597
 Pedicelli S. et al., 2009, *A&A*, 504, 81
 Pilkington K. et al., 2012, *A&A*, 540, A56
 Przybilla N., Butler K., Becker S. R., Kudritzki R. P., Venn K. A., 2000, *A&A*, 359, 1085

- Reetz J., 1999, *Ap&SS*, 265, 171
 Sanchez S. F., Rosales-Ortega F. F., Iglesias-Paramo J. et al., 2014, *A&A*, 563, 49
 Schuler S. C., King J. R., Terndrup D. M., Pinsonneault M. H., Murray N., Hobbs L. M., 2006, *ApJ*, 636, 432
 Scott P., Asplund M., Grevesse N., Sauval J., 2009, *ApJ*, 691, L119
 Sitnova T. M., Mashonkina L. I., Ryabchikova T. A., 2013, *Astron. Lett.*, 39, 126
 Stasinska G., Peña M., Bresolin F., Tsamis Y. G., 2013, *A&A*, 552, 12
 Steenbock W., Holweger H., 1984, *A&A*, 130, 319
 Takeda Y., 1992, *PASJ*, 44, 309
 Takeda Y., Kawanomoto S., Ohishi N., 2007, *PASJ*, 59, 245
 van Regemorter H., 1962, *ApJ*, 136, 906
 Vernazza J. E., Avrett E. H., Loeser R., 1981, *ApJS*, 45, 635
 Yong D., Carney B. W., Friel E. D., 2012, *AJ*, 144, 95

SUPPORTING INFORMATION

Additional Supporting Information may be found in the online version of this article:

Table 1. Parameters and abundances for program Cepheids. (<http://mnras.oxfordjournals.org/lookup/suppl/doi:10.1093/mnras/stu1643/-/DC1>).

Please note: Oxford University Press is not responsible for the content or functionality of any supporting materials supplied by the authors. Any queries (other than missing material) should be directed to the corresponding author for the article.

This paper has been typeset from a $\text{\TeX}/\text{\LaTeX}$ file prepared by the author.